HPV16 Tumor Associated Macrophages Suppress Antitumor T Cell Responses

Ana Paula Lepique,[1] Katia Regina Perez Daghastanli,[2] Iolanda Midea Cuccovia,[2] and Luisa Lina Villa[1]

Abstract

Purpose: High-risk human papillomavirus (HPV) is the main etiologic factor for cervical cancer. The severity of HPV-associated cervical lesions has been correlated to the number of infiltrating macrophages. The objective of this work is to characterize the role of tumor-associated macrophages (TAM) on the immune cellular response against the tumor.

Experimental Design: We used the HPV16 E6- and E7-expressing TC-1 mouse tumor model to study the effect of TAM on T-cell function *in vitro*, and depleted TAM, using clodronate-containing liposomes, to characterize its role *in vivo*.

Results: TAM, characterized by the positive expression of CD45, F4/80, and CD11b, formed the major population of infiltrating tumor cells. TAM displayed high basal Arginase I activity, producing interleukin-10 (IL-10); they were resistant to iNOSII activity induction, therefore reversion to M1 phenotype, when stimulated *in vitro* with lipopolysaccharide/IFNγ, indicating an M2 phentoype. In cultures of isolated TAM, TAM induced regulatory phenotype, characterized by IL-10 and Foxp3 expression, and inhibited proliferation of CD8 lymphocytes. *In vivo*, depletion of TAM inhibited tumor growth and stimulated the infiltration of tumors by HPV16 $E7_{49-57}$-specific CD8 lymphocytes, whereas depletion of $Gr1^+$ tumor-associated cells had no effect.

Conclusions: M2-like macrophages infiltrate HPV16-associated tumors causing suppression of antitumor T-cell response, thus facilitating tumor growth. Depletion or phenotype alteration of this population should be considered in immunotherapy strategies.

Human papillomavirus (HPV), the main etiologic factor for cervical cancer, is detected in 99.7% of the tumor cases (1). Epidemiologic evidence shows that HPV is the causal agent in a significant percentage of other genital tumors (2). HPV16, the most prevalent type, is present in 50% of cervical tumors throughout the world (2). Although most women clear the infection within two years, some sustain persistent infection, which correlates with increased risk of cancer development (3, 4). Cancer is the final step of a long natural history preceded by the infection itself, infection persistence, and integration of the viral genome (5, 6).

Persistent infection requires immune tolerance, and HPV, mainly via the E6 and E7 oncoproteins, has evolved several evasion mechanisms such as absence of inflammation (7–12), production of regulatory cytokines (i.e. transforming growth factor β; ref. 8), disruption of IFN type I–responsive pathways (9, 10), and down-regulation of TLR9 expression (11). The immune responses of the host against HPV antigens eliminate most of the infections and promote lesion regression, probably through a CD4 Th1 response against the proteins E2, E6, and E7 (13). Interestingly, women bearing HPV-associated tumors not only have weak CD4 responses (13, 14), but also display regulatory ones from lymphocytes stimulated with HPV antigens (15). In addition, a positive correlation was found between the number of $CD68^+$ macrophages in cervical disease and lesion grade (16, 17). Increasing evidence indicates that tumor-associated macrophages (TAM) and other myeloid-derived cells have important roles in tumor progression in several models (18–21). These myeloid cells secrete regulatory cytokines such as interleukin 10 (IL-10) and transforming growth factor β, have high Arginase I activity, and induce a regulatory phenotype or cell death on lymphocytes (18, 19). On the other hand, M1 macrophages exhibit cytotoxic function and are involved in antitumor activity either directly (22, 23) or by activation of natural killer and T cells (24).

In the present study, we investigated the role of macrophages in HPV16-induced tumors using the E6/E7-expressing TC-1 tumor model (25–28). Complementary methods were used to show that $CD45^+CD11b^+F4/80^+$/$Arginase1^+IL10^+$ M2 macrophages (TAM) are the main population of immune cells infiltrating TC-1 tumors. Depletion of this population using clodronate-containing liposomes inhibits tumor growth, and enhances tumor-specific CD8 T-cell responses. Our results clearly indicate that TAM facilitate tumor growth by inhibiting antitumor T-cell function.

Authors' Affiliations: [1]Laboratory of Virology Ludwig Institute for Cancer Research, São Paulo branch, Rua João Julião, 245, and [2]Instituto de Química, Universidade de São Paulo, Departmento de Bioquímica, Av. Prof. Lineu Prestes, São Paulo, SP, Brazil

Received 2/25/09; accepted 3/30/09; published OnlineFirst 6/23/09.

Grant support: Fundação de Amparo à Pesquisa do Estado de São Paulo (FAPESP), process 04/00749-2.

The costs of publication of this article were defrayed in part by the payment of page charges. This article must therefore be hereby marked *advertisement* in accordance with 18 U.S.C. Section 1734 solely to indicate this fact.

Note: Supplementary data for this article are available at Clinical Cancer Research Online (http://clincancerres.aacrjournals.org/).

Requests for reprints: Ana Paula Lepique, Ludwig Institute for Cancer Research, São Paulo branch, Rua João Julião, 245, 1st floor, 01323-903, São Paulo, SP, Brazil. Phone: 55-11-35490461; Fax: 55-11-32844966; E-mail alepique@ludwig.org.br.

doi:10.1158/1078-0432.CCR-09-0489

Translational Relevance

Increasing evidence has indicated that tumor-associated macrophages promote tumor growth by inducing angiogenesis or by suppressing antitumor T-cell responses. In human papillomavirus (HPV)-associated cervical lesions, increasing numbers of infiltrating macrophages correlate with higher-grade lesions. The main proteins mediating immune evasion and tumor growth in HPV-associated tumors are the oncoproteins E6 and E7. In this work we used a tumor model that expresses both E6 and E7 proteins from HPV16 to characterize the tumor-infiltrating macrophage population. We observed that these cells have an M2-like profile and that they induce a regulatory phenotype in T cells and inhibit antigen-driven lymphoproliferation.

We used clodronate-containing liposomes to deplete these macrophages from tumors in mice, both before and after tumor establishment, and observed increased antitumor responses and tumor growth inhibition. Depletion, via local liposome application or manipulation of this population, should be considered in immunotherapy against HPV-associated lesions.

Materials and Methods

Cell line, mice, and reagents

The TC-1 cell line was kindly donated by Dr. TC Wu, John Hopkins, Baltimore (25). Cells were maintained in 10% FCS in RPMI supplemented with 400 μg/mL neomicin at 37°C and 5% CO_2 atmosphere. For mouse injections, 10^5 cells were suspended in 100 μL of 0.5 mmol/L $MgCl_2$, 1 mmol/L $CaCl_2$ PBS. All mice were injected with 10^5 cells s.c. in the right dorsal flank.

C57Black/6 mice were maintained in specific pathogen-free conditions, with 12 h light/dark cycles. All procedures using mice were approved by the Ethical Animal Care and Use Committee, Fundação Antônio Prudente (Project 018/07).

Disodium clodronate (Rhodia Pharma) was used without further purification. Egg phosphatidylcholine was prepared as described (29). Cholesterol (Sigma-Aldrich) was recrystallized from methanol/acetate. Mouse recombinant IFNγ was from Peprotech, and lipopolysaccharide (LPS; *Escherichia coli* endotoxin serotype 0111:B4; Sigma-Aldrich) was kindly donated by Dr. Adriana A. Dias, Fundação Antônio Prudente (Brazil). Carboxyfluorescein diacetate succinimidyl ester and propidium iodide were from Invitrogen. PE-conjugated K^d $HPV16E7_{49-57}$ and irrelevant tetramers were provided by Dr. Philippe Guillaume and Dr. Immanuel Luescher (Ludwig Institute for Cancer Research, Switzerland). The antibodies, with the respective clones in parentheses, used throughout this work were CD3e (145-2C11), CD4 (GK1.5), CD8 (53-6.7), F4/80 (6F12), Gr1 (RB6-8C5), CD16/32 (2.4G2), CD19 (1D3), CD45 (30-F11), TCRγδ (GL3), IFNγ (XMG1.1), Arginase I (19), and iNOSII (6) from BD Biosciences; F4/80 (BM8) and Foxp3 (FJK-16s) from eBiosciences; CD11b (M1/70) from R&D Systems; and IL-10 (JES5-16E3) from Miltenyi Biotec.

Cell preparations

All cell preparations were made using 1× Hanks' solution with 15 mmol/L HEPES pH 7.4, 0.5 U/mL DNase (Worthington) and 5% fetal bovine serum. Spleen suspensions were obtained by tissue dissociation through a 70-μm metal mesh and red cell lyses in hypotonic buffer. Tumor suspensions were obtained by digestion of minced tissue with 0.5 mg/mL collagenase I, in a Thermomixer (Eppendorf). Cell viability in the final suspensions was between 90% and 95%.

Flow cytometry

Single cell suspensions were stained with different antibodies (indicated in each figure) after blocking with anti-CD16/CD32 at 0.5 ug/10^6 cells for 15 min. All cell cytometry acquisition and analyses were done in a FACScalibur, using the CellQuest software (BD Biosciences).

Immunohistochemistry and immunofluorescence

Acetone/methanol (2:1 v/v)-fixed 5-μm cryosections were blocked with 5% fetal bovine serum in PBS, together with, when necessary, 1 mg/mL rat IgG and 0.5 μg/mL anti-CD16/CD32 for 30 min at room temperature prior to incubation with primary antibodies. The ABC Vectastain kit (Vector Laboratories) was used for immunohistochemistry, followed by Mayer's hematoxylin counterstaining and slide mounting in Permount (Fisher Scientific). For fluorescence, fluorochrome-conjugated antibodies were incubated for 30 min after blocking. Tetramers were incubated overnight at 4°C. Tissue was counterstained with 4′6-diamidino2-phenylindole (Sigma-Aldrich). Slides were mounted with Prolong (Invitrogen). Images were obtained with an IX70 Olympus fluorescence microscope (Olympus, Corp.), a DP70 Olympus camera, using its own software.

For ArginaseI and iNOSII immunocytochemistry, cells seeded in Labteks were fixed in buffered 4% formaldehyde, permeabilized with 0.1% Triton X100, 5% fetal bovine serum in PBS, and treated as above.

Cell sorting

Cells were stained for flow cytometry and sorted either in a FACSCalibur or using magnetic beads conjugated with antibodies against the fluorochrome EasySep system (Stem Cell Technologies). In general, we obtained 98% viable cells with at least 95% purity. For fluorescence-activated cell sorting, we used propidium iodide staining for dead cell exclusion.

Arginase and iNOSII activity

Arginase activity assay in total cell lysates was done as previously described (30). For iNOSII activity, cells were seeded in 96-well culture dishes in 10% RPMI and incubated at 37°C for 2 h. Adherent cells were treated with 100 U/mL IFNγ (Peprotech) and 10 ng/mL LPS for 12 h. Supernatants were then harvested for nitrite detection by Griess test (31). Aliquots of cell lysates were used for protein quantification by the Bradford assay (BioRad; ref. 32).

Mouse immunization

Mice were immunized with three doses of 100 μg of purified HPV16 E7 recombinant protein or three doses (25 μg each) of purified HPV16 $E6_{48-57}$ and $E7_{49-57}$ peptides (kindly provided by Dr. Maria Juliano, Universidade Federal de São Paulo, Brazil) at days 0, 15, and 45. One hundred micrograms of oligonucleotide 1826ODN was used as adjuvant. The E7 recombinant protein was expressed from a construction of *HPV16 E7* complete gene in the pET28a system in BL21 bacteria after 24 h induction with 1 mmol/L isopropyl-β-D-thiogalactopyranoside. The recombinant protein was purified with the His-trap FF system (GE Healthcare) according to the manufacturer's instructions. Eluted fractions were analyzed for E7 expression by Western blotting, using a specific anti-E7 antibody (Invitrogen).

T cell functional assays

T cells from lymph nodes from HPV16 E7-immunized C57B/6 mice were cocultured with $CD11b^+$ splenocytes or $CD45^+$ cells from TC-1 tumors in a 4 lymphocyte:1 myeloid cell proportion. HPV16 E7 protein (10 ug/mL) was used as antigen. For cytokine staining we used the GolgiStop Fixation/Permeabilization kit following the manufacturer's instructions (BD Biosciences); Foxp3 staining was done in fixed and permeabilized cells; for apoptosis detection we used FITC-conjugated Annexin V (University of São Paulo). Carboxyfluorescein diacetate succinimidyl ester–labeled T cells were used in lymphoproliferation studies with total adherent splenocytes as antigen-presenting cells.

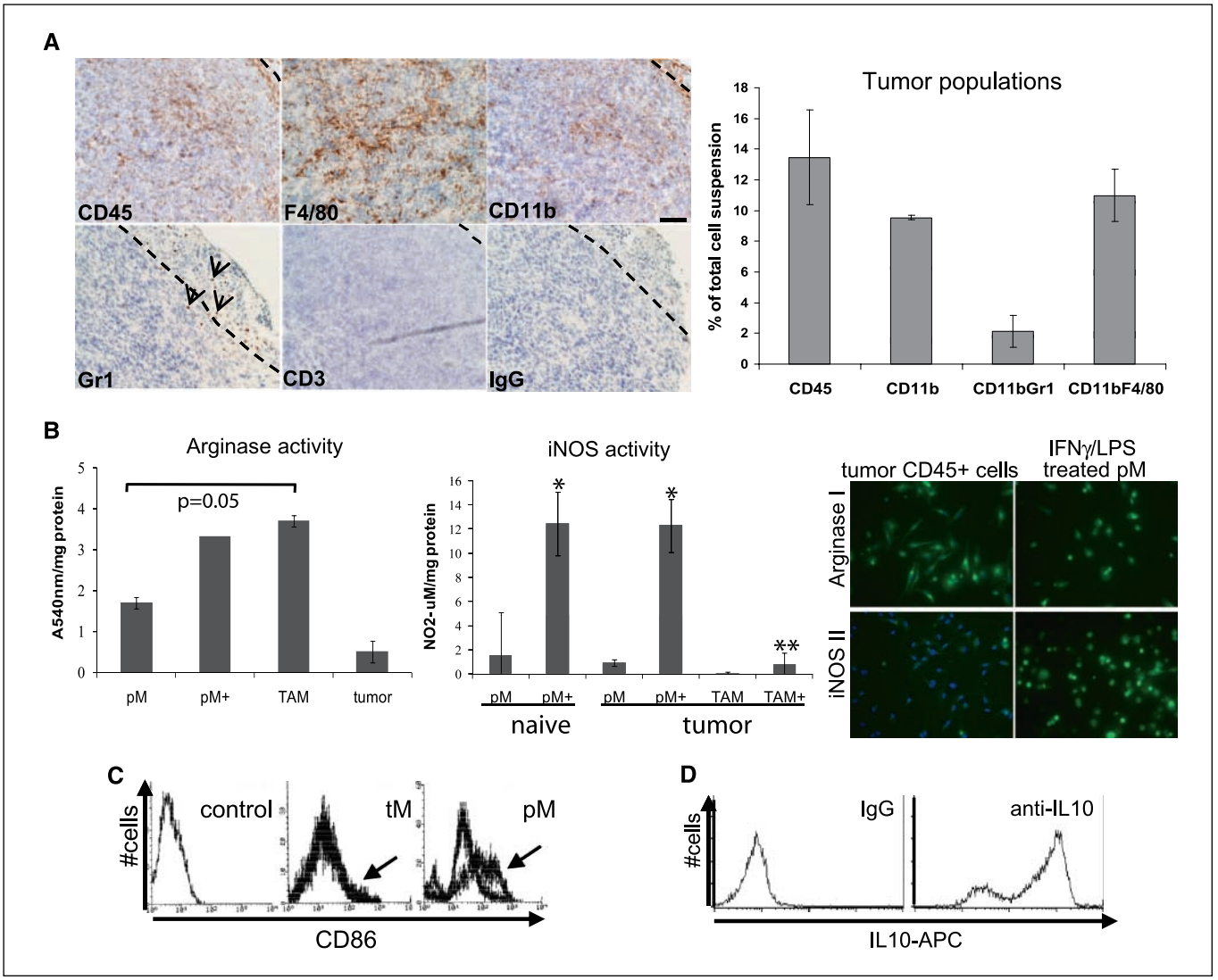

Fig. 1. TC-1 tumor infiltrate characterization. *A,* left panels, immunohistochemistry of tumor cryosections showing localization of total leukocytes (CD45), myeloid cells (CD11b and Gr1), macrophages (F4/80), and T cells (CD3). Dotted lines highlight the tumor/capsule border, except the F4/80 panel, where we chose a central area to exemplify this population distribution. IgG, isotype control. Magnification ×200. Scale bar, 100 μm. Right graph, total tumor cell suspension flow cytometry analysis from tumors harvested 2 to 3 wk post – TC-1 injection. Cells were stained with antibodies against the indicated markers; 30,000 events were acquired per sample. Results represent the average of 10 mice. *B,* arginase and iNOS activities (*graphs*) and expression (*right panels*) in sorted cell lysates or cell supernatants from naive and tumor-bearing mice. Horizontal axis, peritoneal macrophages (pM) and tumor isolated macrophages (TAM); +, treatment with 100 ng/ml LPS/100 U/ml IFNγ for 16 h. Results are the average of cells harvested from at least six mice. Significant differences are indicated by * (treated × untreated pM) and ** (treated TAM and pM). Micrographs represent Arginase I and iNOSII expression in $CD45^+$ sorted from TC-1 tumors. Positive controls are resident peritoneal macrophages stimulated as described in *C* and *D* (IFNγ/LPS-treated pM). Magnification ×400. Scale bar, 50 μm. *C* and *D,* cell cytometry analysis. *C,* CD86 expression in tumor (tM) and peritoneal macrophages (pM), stimulated (*arrows*) as described in *B. D,* IL-10 expression in CD45+ tumor isolated cells. Controls are cells incubated with isotype antibody, 10,000 events were acquired per sample.

Liposome preparation

Clodronate was entrapped in liposomes by ether injection as described (33). Typically, 0.5 mL of an ethereal solution containing 50 mg phosphatidylcholine, and 8 mg cholesterol were injected (0.2 mL/min) into 5 mL of a 50 mmol/L clodronate aqueous solution maintained at 42°C. The ethereal solution was injected with a syringe adapted in a KD Scientific Inc. Model KDS120 Push-Pull Pump, equipped with a fine-gauge needle (No 3D). During injection, an N_2 stream was bubbled into the clodronate solution, which continued after liposome formation until removal of residual solvent. The liposome suspension was centrifuged at 22800 *g* for 30 min (Hitachi Himac CR20B2 centrifuge; Hitachi Ltd.) at 25°C. The liposome-containing pellet was washed twice, by centrifugation under the same conditions, in saline solution. All the times saline is mentioned in the text it is a 0.9% (w/v) NaCl solution. The final pellet was resuspended in 2 mL of saline solution and filtered through a 0.8 μm polycarbonate membrane. Clodronate concentration in aqueous phase was determined as described (34). Phosphatidylcholine concentration was determined as described (35). Typically, the final phosphatidylcholine and clodronate concentrations in the liposomes were 10 mmol/L and 0.5 mmol/L, respectively. The yield of entrapped clodronate was about 1% of the initial quantity added, 60 μg per mL of preparation.

Clodronate-containing liposome treatment and tumor growth kinetics

Depletion of macrophages before tumor growth. Mice were injected i.p. with 200 μL of liposome preparation (12 μg of clodronate), 24 h later injected s.c. with a mix of 10^5 TC-1 cells and 100 μL of liposome preparation (6 μg of clodronate), and 7 d later with another 100 μL dose of liposome preparation near the tumor cell injection site.

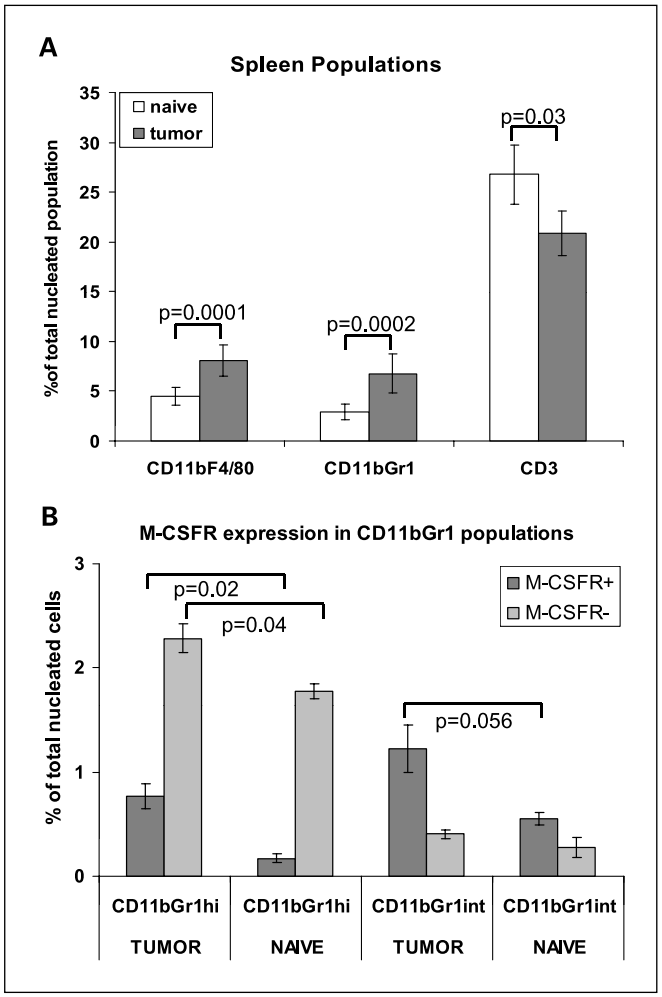

Fig. 2. Flow cytometry analysis of spleen cell populations. Nucleated single cell suspensions from spleens of naïve (*white bars*) or tumor-bearing mice (*gray bars*) were stained with antibodies against the indicated cell markers. *A,* comparison of myeloid and T cell populations; results are the average of 10 mice. Significant differences are indicated by *P* values in the graph; 30,000 events per sample were acquired. *B,* expression of M-CSFR in subsets of $CD11b^+Gr1^+$ population. Cells were stained with anti-CD11b, Gr1 and M-CSFR; $Gr1^{hi}$ and $Gr1^{int}$ populations were gated separately for M-CSFR expression analyzes. Significant differences are indicated (*t*-test); 50,000 events per sample were acquired.

Depletion of macrophages after tumor establishment. TC-1 cells (10^5) were injected s.c. in the dorsal flank of mice. When the tumors were palpable (3-4 mm in the largest diameter), the mice received two doses of 100 μL each of liposome preparation with a 1-wk interval, near the tumor site. One week later the tumors were harvested for analysis.

Statistical analysis

Tumor growth kinetics experiments were tested by the Mann-Whitney *U*-test and by Student's *t*-test, when comparing groups at specific time points. All other experiments were tested by Student's *t*-test, comparing data between two groups. In all cases, $P < 0.05$ was considered significant.

Results

$CD45^+CD11b^+F4/80^+Arginase I^+$ macrophages are the main population infiltrating TC-1 tumors. Two to three weeks after inoculation of TC-1 cells, immunohistochemical analysis showed tumor infiltration by $F4/80^+$, $CD11b^+$, and/or $Gr1^+$ leukocytes, whereas $CD3^+$ lymphocytes were rarely found (Fig. 1A, micrographs). The $CD45^+$ leukocyte population represented 13.5 ± 3% of all cells in the tumor (Fig. 1A, *right panel*). $CD11b^+F4/80^+$ macrophages (TAM) were predominant (11 ± 1.7% of all tumor cells), whereas $CD11b^+Gr1^+$ macrophages corresponded to 2.12 ± 1% of all cells in the tumor (Fig. 1A). Notably, the $CD11b^+F4/80^+$ tumor-associated macrophages were actually infiltrating the TC-1 tumor cell nests and were seen all over the tumor area (Fig. 1A; F4/80, micrograph representing the central tumor area), whereas $Gr1^+$ cells were concentrated in the capsule and tumor periphery (Fig. 1A; Gr1, *arrows*).

Both $CD45^+$ and $CD45^+F4/80^+$ cells were characterized after sorting from TC-1 tumors. TAM were either immediately lysed to measure Arginase activity or stimulated with 100 U/mL IFNγ/100 ng/mL LPS to activate iNOS. TAM Arginase activity was higher than that of nonstimulated peritoneal macrophages (pM) and similar to the activity of *in vitro* – activated peritoneal macrophages (pM^+; Fig. 1B, *left panel*). The CD45-negative tumor cell population (tumor) displayed very low Arginase activity (Fig. 1B, *left panel*). TAM did not display iNOS activity even after activation with 100 U/mL IFNγ/10 ng/mL LPS (Fig. 1B, *middle panel*). In contrast, peritoneal macrophages harvested from either tumor-bearing or naïve mice displayed an 8-fold increase in iNOS activity after stimulation (Fig. 1B, *middle panel*). Immunocytofluorescence assays confirmed that unstimulated TAM expressed Arginase I and did not express iNOSII (Fig. 1B, *right panels*). The controls for antibody reactions were activated peritoneal macrophages as described above (Fig. 1B, *right panels*). Stimulation of TAM with IFNγ/LPS did not induce CD86 expression (Fig. 1C; *arrows*, LPS/IFNγ treated cells), and IL-10 was expressed independently of stimulation, as measured by intracellular staining (Fig. 1D). Collectively, these data indicate that the main population of HPV16-associated TC-1 tumor-infiltrating immune cells are M2-like macrophages, resistant to IFNγ/LPS treatment. This finding corroborates previous data in other types of tumors (36–38).

Myeloid populations are expanded in the spleen of tumor-bearing mice. The spleens of tumor-bearing mice were hypercellular, with 127.5 ± 10.75 million nucleated cells, compared with naïve mice with 70 ± 8 million nucleated cells. There was a 2-fold increase in the numbers of $CD11b^+Gr1^+$ and $CD11b^+F4/80^+$ populations in tumor-bearing mice, whereas the percentage of T cells was somewhat decreased (Fig. 2A). Within the $CD11b^+Gr1^+$ population, the $Gr1^{int}$ represents myeloid-derived cells and $Gr1^{hi}$ granulocytes (39). We observed expansion of both subsets, and still within these, higher number of cells expressing MCSF-R, a suppressor marker (39), in splenocytes tumor-beating mice (Fig. 2B). Altogether our data suggest that the outgrowth of HPV16+ TC-1 tumors results in the expansion and infiltration of macrophage populations that, according to their phenotypes, are potential suppressors of T-cell function.

Myeloid cells from HPV16-associated tumor model TC-1 induce regulatory phenotype on T cells. In other tumor models, myeloid populations expanded in tumors are able to induce regulatory phenotype on T cells, suppressing the antitumor response (19, 40).

The immunomodulatory capacity of myeloid cells in TC-1 tumor – bearing mice was evaluated *in vitro*. Sorted $CD45^+$ TAM as well as $CD11b^+$ and $Gr1^+$ splenocytes, pulsed with

recombinant E7 protein, were antigen-presenting cells. Lymph node–derived lymphocytes from HPV16 E7–immunized mice were the responder cells. CD11b$^+$ splenocytes from naïve mice were used as controls. Upon stimulation of responder cells with control CD11b$^+$ cells, 10% of the CD4 T cells and 14% of the CD8 cells produced IFNγ (Fig. 3A; *upper panels*, CD11bN), and no IL-10 expression induction was observed (Fig. 3A; *lower panels*, CD11bN). CD11b$^+$ cells from tumor-bearing mice efficiently induced IFNγ production by CD4 and CD8 T cells (Fig. 3A; *upper panels*, CD11bT), although with a significant decrease in their capacity to stimulate IFNγ by CD8 T cells (8.7 ± 1%; Fig. 3A; CD11bT, *right upper panel*). The percentage of IFNγ-producing lymphocytes in cocultures with Gr1$^+$ cells was similar to that of the nonstimulated control samples (Fig. 3A; *upper panels*, Gr1T). Lymphocytes incubated with TAM were virtually negative for IFNγ expression (Fig. 3A, *upper panels*). In

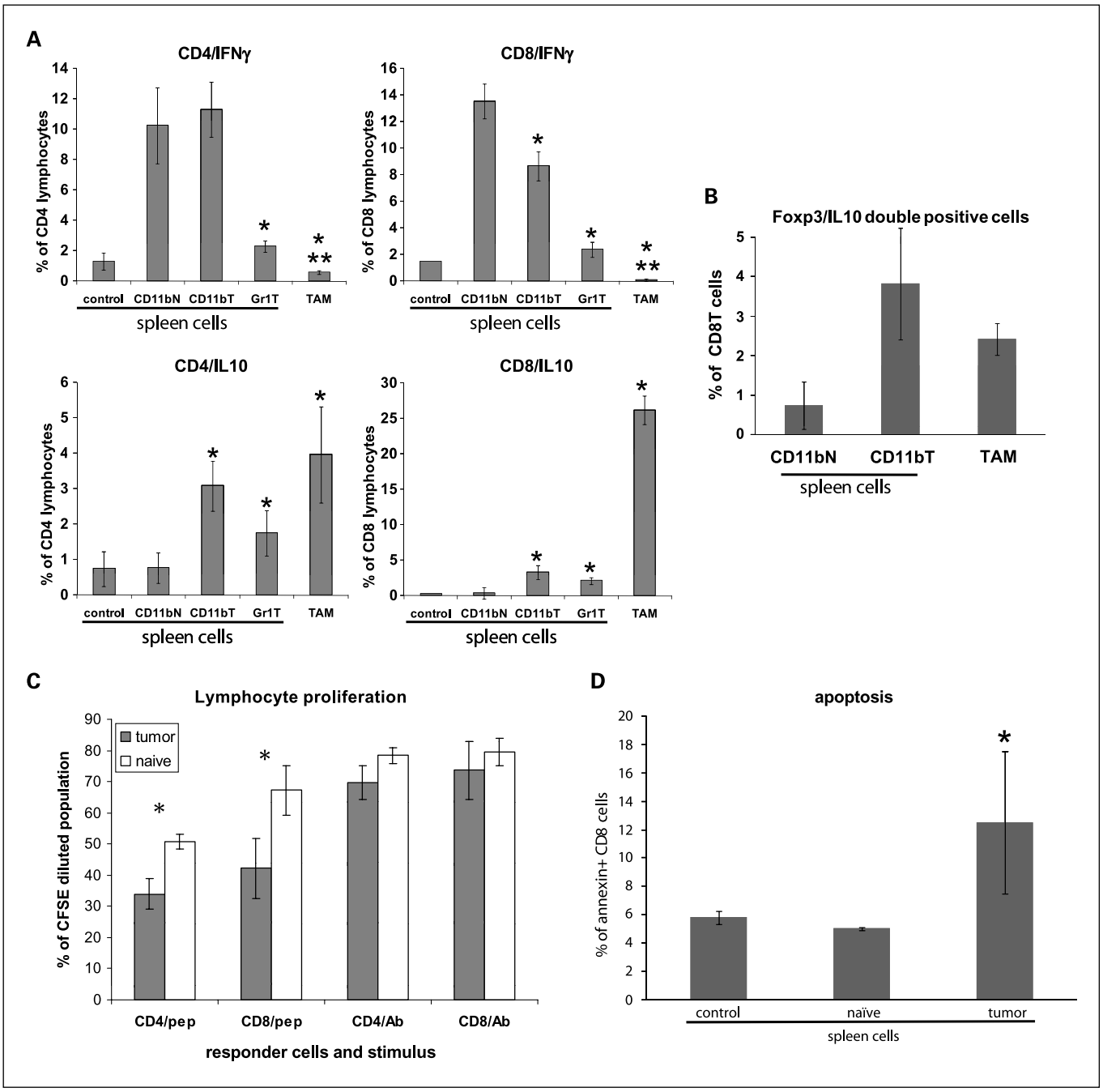

Fig. 3. Effect of myeloid populations on T-cell functions. *A, B,* and *D,* abscissas indicate antigen-presenting populations: CD11b$^+$ splenocytes from naïve (CD11bN) or tumor bearing mice (CD11bT), Gr1$^+$ splenocytes of tumor-bearing mice (Gr1T), or CD45$^+$ TC-1 isolated tumor cells (TAM) loaded with 50 μg of E7 recombinant protein; control are unloaded cells. *A,* ordinates indicate percentages of CD4 and CD8 lymphocytes expressing IFNγ or IL-10, as indicated on the top of each graph, measured by flow cytometry. *B,* coexpression of IL-10 and Foxp3 on CD8 lymphocytes measured by intracellular staining and flow cytometry analysis. *C,* lymphoproliferation measured by carboxyfluorescein diacetate succinimidyl ester dilution in responder cells stimulated with 15 μg of $E7_{49-57}$ peptide (pep) or with 0.5 μg/mL anti-CD3 and anti-CD28 (Ab). *D,* CD8 apoptosis rate in cocultures as previously described and measured by Annexin V binding and flow cytometry analysis where 50,000 events gated on lymphocyte population were acquired. *, significant differences between each population and the naïve control; **, significant differences between the populations and unstimulated control.

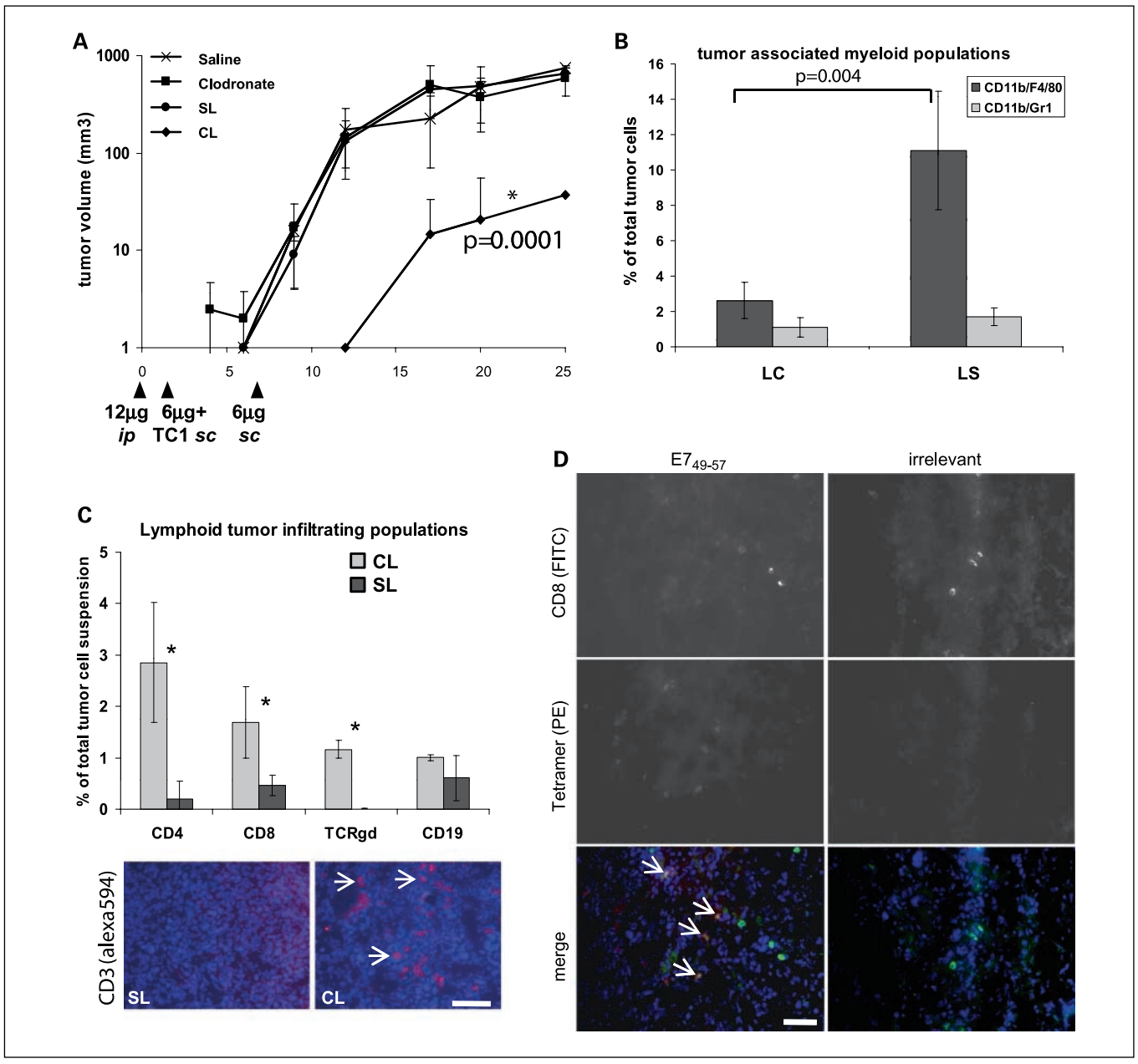

Fig. 4. Effects of CL treatment on TC-1 tumors. *A,* tumor growth kinetics in mice treated as indicated: Saline (0.9% w/v NaCl), Clodronate, indicated dose diluted in saline; SL, saline containing liposomes; CL, clodronate containing liposomes, indicated doses. Data represent the average of 10 mice per group. Significant differences between CL-treated mice and other groups was $P < 0.0001$ by Mann-Whitney U test. *B* and *C,* flow cytometry analysis and immunofluorescence of tumor infiltrate (results are the average of six mice). *B,* myeloid population phenotype and significant differences are indicated in the graph. *C,* upper panel, lymphocyte populations in total tumor cell suspensions. All differences between SL and CL were significant, except for the B cell population. Lower panels, immunofluorescence for CD3 in tumor cryosections. Tissue sections were counterstained with 4′6-diamidino2-phenylindole. Magnification 600× (40× objective, plus 1.5× in the microscope). *D,* immunofluorescence for CD8 and tetramers in cryosections of tumors. Sections were stained with FITC-conjugated anti-CD8 and the indicated tetramers conjugated to PE. 4′6-diamidino2-phenylindole was used for counterstaining. Arrows, double positive cells. This experiment is representative of three independent ones. Magnification ×400. Scale bars, 50 µm.

contrast, E7-specific CD4 T cells (4 ± 1.5%) and CD8 T cells (26.18 ± 2%) produced IL-10 upon stimulation with E7-pulsed TAM (Fig. 3A, *lower panels*). In addition, $CD11b^+$ and $Gr1^+$ cells derived from tumor-bearing animals significantly stimulated IL-10 production in CD4 and CD8 lymphocytes when compared with controls (Fig. 3A; *lower panels*, CD11bT and Gr1T). In view of the IL-10 production by CD8 lymphocytes, reminiscent of CD8 regulatory T cells (41), we analyzed the expression of Foxp3 in this T cell population. Simultaneous expression of IL-10 and Foxp3 was found in 2.4% of CD8 T cells stimulated with TAM and in 3.8% of CD8 T cells stimulated with $CD11b^+$ splenocytes from tumor-bearing mice (CD11bT; Fig. 3B).

The immunomodulatory capacity of myeloid cells in tumor-bearing mice on antigen-specific–driven lymphoproliferation was tested. There was a 40% reduction in proliferation in response to E7 when T cells were stimulated in the presence of splenocytes from tumor-bearing mice (Fig. 3C). This reduction may be related to enhanced apoptosis as we detected a 2.4-fold higher apoptosis rate in CD8 lymphocytes incubated with $CD11b^+$ cells from tumor-bearing mice when compared with

$CD11b^+$ cells from naïve mice (Fig. 3D; tumor and naïve, respectively). Apoptosis was not measured in cocultures with TAM, because the latter displayed a high background when probed with Annexin V. Overall, these results indicate that TAM and splenic myeloid cells from tumor-bearing mice suppress CD4 and CD8 T-cell responses by inducing a regulatory phenotype in these cell populations and by lowering their proliferative capacity, possibly by inducing apoptosis.

Macrophage depletion delays HPV16-associated tumor growth and allows tumor infiltration by lymphocytes. Modulation of activity of myeloid-derived cells or TAM may reduce tumor growth and stimulate antitumor T cell responses (24, 42).

We evaluated the role of TAM *in vivo* by depletion with clodronate-containing liposomes (CL; ref. 43). Clodronate reacts with ATP generating methylene containing ATP analogs, which induces cell death if accumulated in the cell cytoplasm (44). CL did not affect the viability of TC-1 tumor cells *in vitro* or *in vivo* (Supplementary Fig. S1). Macrophages were depleted by an i.p. injection of CL 24 hours before the s.c. injection of 10^5 TC-1 cells and another dose of liposomes. One week later, the mice received a peritumoral s.c. dose of CL (Fig. 4A). Control mice were treated with saline, clodronate in aqueous solution, or saline-containing liposomes (SL). In CL-treated mice palpable tumors were detected one week after the last treatment dose (Fig. 4A). The differences in tumor growth kinetics between CL-treated mice and controls were highly significant (P = 0.0001 by Mann-Whitney; P = 0.001 by Student's t-test comparing CL-treated mice against any other group, at each kinetic time point). Furthermore, a robust change in tumor infiltrate was observed in CL-treated mice as compared with SL treatment. In CL-treated mice TAM represented 2.6 ± 1% of the total tumor cells, whereas in SL-treated mice, these cells represented 11.1 ± 3.3% of the total tumor population (Fig. 4B). No difference in the tumor-associated $CD11b^+Gr1^+$ population was observed between treatments (Fig. 4B). CL treatment resulted in an increase of tumor infiltration by lymphocytes: 2.8% of CD4 lymphocytes, 1.8% of CD8 lymphocytes, and 1% TCRγδ T cells related to total tumor cells (Fig. 4C, *upper panel*). In contrast, lymphocyte infiltration was <0.5% of the tumor cells in control-treated mice. Immunofluorescence of tumor cryosections stained with anti-CD3 revealed a similar pattern (Fig. 4C, *lower panels, arrows*). As TC-1 presents the dominant MHC class I–restricted CTL epitope HPV16 E7, we assessed whether CL treatment also enhanced tumor infiltration by HPV16 $E7_{49\text{-}57}$-specific C8 T cells. In tumor cryosections stained with anti-CD8 and MHC-I $E7_{49\text{-}57}$tetramer, E7-specific CD8 T cells were detected only when mice were treated with CL (Fig. 4D, *left panels, arrows*). We did not observe binding of irrelevant tetramer to the tumor tissue (Fig. 4D).

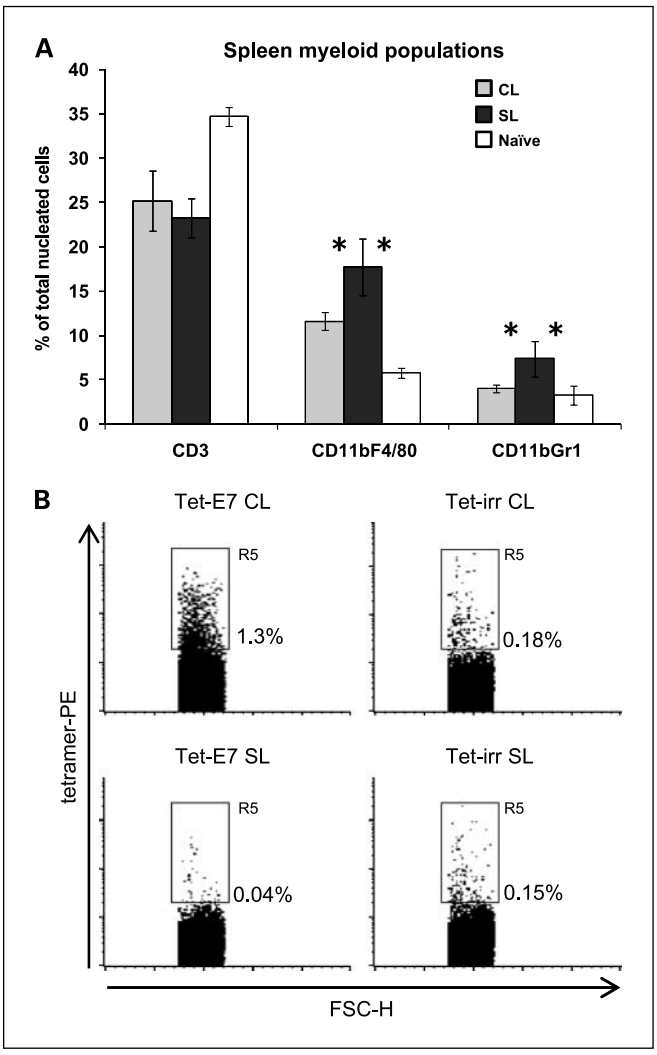

Fig. 5. Effect of CL treatment on spleen populations. *A,* flow cytometry analysis of nucleated single cells from spleens of naïve, CL-treated, and LS-treated mice. Cells were stained for the indicated markers; 30,000 events per sample were acquired. Results are the average of data obtained from six mice. *, significant difference (t-test). *B,* detection of E7 specific population in the spleen. CD8 splenocytes were incubated with PE-conjugated tetramers HPV16 $E7_{49\text{-}57}$ or loaded with an irrelevant peptide and analyzed by flow cytometry. Left panels, cells stained with E7 peptide loaded tetramers; right panels, with an irrelevant peptide. CL, clodronate liposomes; SL, saline liposomes – treated mice.

In addition, the effect of liposome treatment on spleen populations was investigated. At one week after treatment, when tumors became palpable but were very small, the mice treated with CL displayed a significant reduction of both the $CD11b^+F4/80^+$ and $CD11b^+Gr1^+$ cells in their spleen when compared with SL-treated mice (Fig. 5A). Simultaneously, an expansion of MHC-I $E7_{49\text{-}57}$tetramer-positive CD8 T cell population was observed (Fig. 5B). Notably, when tumors grew larger, we failed to detect E7-specific CD8 T cells in the spleen; however, they were still detected in the tumors of these CL-treated mice, suggesting that they were attracted to the growing tumor.

Macrophage depletion was also investigated in mice with established tumors. Mice were treated with two doses of CL with a one-week interval, and one week later, tumor size and infiltrate were analyzed as described before. Similar to what we observed when macrophages were depleted before tumor challenge, the tumors of CL-treated mice were significantly smaller than in control mice (Fig. 6A), and displayed a significant decrease in TAM (Fig. 6B) and an increase towards detectable numbers of tumor-specific CD8 lymphocytes (Fig. 6C, *solid arrows*). Tumor-isolated TAM displayed no basal iNOS activity (not shown) and decreased Arginase activity (Fig. 6D).

As CL treatment affected the $F4/80^+$ TAM population, we assessed the contribution of $Gr1^+$ cells by depletion with functional anti-Gr1 antibody. Mice were treated with an i.v.

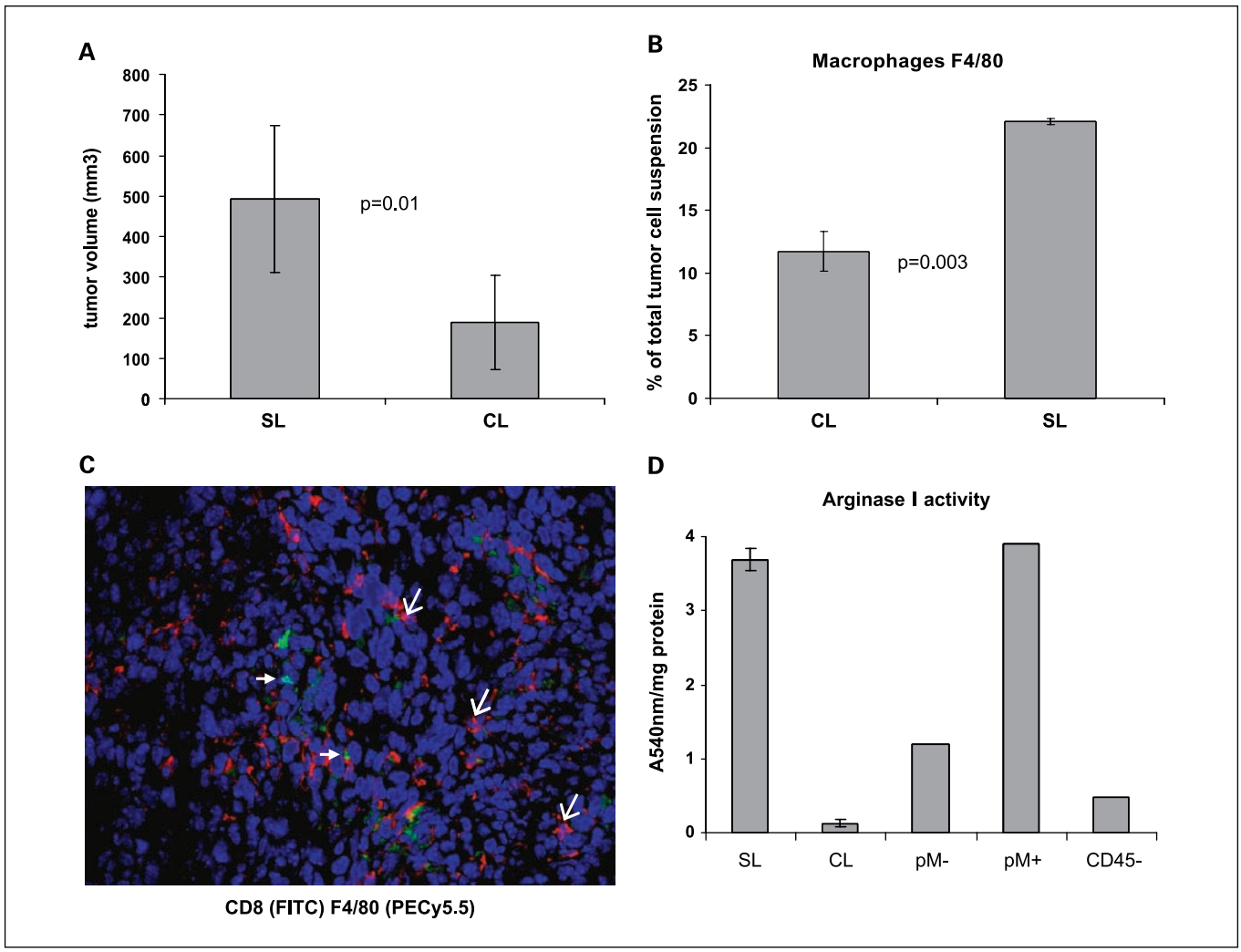

Fig. 6. Effect of CL treatment on established tumors. *A,* tumor volume after harvesting. Results are the average of five mice per group. *B,* total tumor cell suspensions stained with anti-CD45, anti-F4/80, and anti-CD11b, and analyzed by flow cytometry; 30,000 events per sample were acquired. Results are the average of five mice; significance is indicated. *C,* immunofluorescence of a tumor cryosection from a CL-treated mouse stained with FITC-conjugated anti-CD8 (*solid arrows*) and PE/Cy5.5 conjugated anti-F4/80 (*open arrows*), cell nuclei are stained with 4′6-diamidino2-phenylindole. *D,* arginase activity in sorted TAM. pM, untreated; pM+, 100 U/mL IFNγ/100 ng/mL LPS treated peritoneal macrophages. CL and SL tumor macrophages from mice treated with clodronate and saline liposomes, respectively. CD45- tumor cells. Results are the average of three mice.

dose of 100 μg of anti-Gr1 or irrelevant IgG and 24 hours later injected with TC-1 cells. Subsequently, the mice received another three doses of 50 μg of antibody, with an interval of four days between doses (Supplementary Fig. S2A). No differences in tumor volume were observed between anti-Gr1 and IgG-treated mice when the experiment was terminated 16 days post–TC-1 injection. $Gr1^+$ depletion was effective, as can be evidenced by the staining of cryosections of tumors showing few $Gr1^+$ cells in the anti-$Gr1^+$–treated group, whereas $Gr1^+$ cells were distributed as expected, in the capsule and most external areas of the tumor, in control-treated mice (Supplementary Fig. S2B, *arrows*). These results suggest that the $CD11b^+Gr1^+$ macrophage population infiltrating TC-1 tumors was not as significant for tumor growth as TAM.

Discussion

TAM constitute a link between the innate and adaptative responses influenced by the tumor microenvironment (21). As macrophages, other myeloid-derived cell populations present in tumors may cause tolerance towards tumor antigens, for example, by inducing specific regulatory T-cell responses (18, 19, 45). Here we have shown that the TC-1 tumor model, transformed by HPV16 E6 and E7 proteins, is infiltrated by a large number of TAM, an M2-like macrophage population $CD45^+F4/80^+CD11b^+$, but also by myeloid-derived cells $CD45^+CD11b^+Gr1^+$. This model was chosen because E6 and E7 mediate the main immune evasion mechanisms displayed by HPV and are widely used in preclinical protocols for therapeutic vaccines against HPV (25–28). TAM from TC-1 tumors displayed high basal Arginase activity, expressed IL-10, and were resistant to IFNγ/LPS induction of iNOS activity and CD86 expression, supporting an M2-like phenotype (45). In parallel, we observed expansion of myeloid cells in the spleen of tumor-bearing mice, including populations positive for M-CSFR, which is a marker of suppressive phenotype in myeloid cells, mainly in $CD11b^+Gr1^{int}$ population (39). In our case, we observed an increase in M-$CSFR^+$ population mainly within the $Gr1^{high}$ cell subset.

Expansion of $CD11b^+Gr1^+$ cells capable of suppressing CD8 T-cell function in the spleens of mice bearing C3 tumors, another HPV16+ tumor model, was previously described (46). In our model, not only the spleen myeloid cells but also TAM induced, with different efficiencies, a regulatory phenotype on lymphocytes, mainly on CD8 T cells by expression of IL-10 and Foxp3. T cell proliferation was partially inhibited and CD8 apoptosis was increased by antigen-presenting splenocytes from tumor-bearing mice. Proliferation inhibition might be due to the higher apoptosis rate or the effect of regulatory lymphocytes (47). No concrete evidence regarding CD8 regulatory cells in cases of HPV infection or associated disease has been described, but IL-10 secreting CD8 regulatory T cells have been found in patients with other types of cancer and with chronic viral infections by HCV and EBV (48, 49). Our results indicate that immune suppression in tumor-bearing mice is due to both tumor-infiltrating and secondary lymphoid organ myeloid populations.

We aimed to confirm the suppressor function of TAM *in vitro*, by depletion of TAM *in vivo*, by using CL. This method has been widely used in animal models (43) and consists of clodronate encapsulated in phosphatidylcholine and cholesterol liposomes, which are phagocyted by macrophages promoting cell death (44). In our study, treatment with CL inhibited tumor growth either when started before tumor cell injection or after tumor establishment. In the first case, we observed tumor growth only after the treatment was interrupted. Clodronate had no toxic effects on TC-1 cells; therefore, we conclude that CL effect was due only to macrophage depletion. Depletion of macrophages led to tumor infiltration by lymphocyte populations, including HPV16 $E7_{49-57}$-specific CD8 lymphocytes. This CD8 population was expanded in the spleens of CL-treated mice, for as long as the CL treatment was maintained and myeloid cell numbers were low. Similar results, although with smaller effects, were observed when mice with established tumors were treated with CL.

As mentioned before, myeloid-derived $CD11b^+Gr1^+$ cells have a role in antitumor suppression in other tumor models (42). Our results indicate that these cells play a minor role in our model. Firstly, in the tumors, we observed that these cells were localized mainly in the fibroblast capsule around the tumor and in the most external tumor areas, whereas TAM were localized all over the tumor. Secondly, we observed that reduction of Gr1+ cells caused no effect on TC-1 tumor growth. Finally, although expanded in the spleens of tumor-bearing mice, *in vitro*, they were less potent to induce IL-10 expression in lymphocytes than $CD11b^+$ cells from the same mice.

We have shown that, *in vitro*, TAM are resistant to treatment with IFNγ and LPS. TAM from E2-K14HPV16 transgenic mice down-regulated the expression of MMP9 upon mice treatment with zolendronic acid (a biphosphonate-like clodronate, but with a different mechanism of action; ref. 50). In a mouse ovarian cancer model, inhibition of the nuclear factor-κB pathway led to macrophage phenotype alteration (24). Whether the phenotype of TC-1 TAM may be altered by the above treatment strategies remains to be established. Our data indicate, however, that depletion of this population may improve the efficacy of therapeutic vaccines. A prolonged CL treatment may be possible, once it is specific and nontoxic to cells other than those that phagocyte the vesicles. We propose that, whether by modification or by depletion, TAM be taken into consideration in immune therapeutic approaches against tumors associated with HPV or other tumors that are infiltrated by similar populations.

Disclosure of Potential Conflicts of Interest

No potential conflicts of interest were disclosed.

Acknowledgments

We thank Dr. Philippe Guillaume and Dr. Immanuel Luescher (Ludwig Institute for Cancer Research, Lausanne, Switzerland) for providing the E7 and irrelevant tetramers, and Dr. Sjoerd van der Burg, (University of Leiden, the Netherlands) and Dr. Hernan Chaimovich Guralnik (Universidade de São Paulo, Brazil) for the critical reviewing of the manuscript.

References

1. Walboomers JM, Jacobs MV, Manos MM, et al. Human papillomavirus is a necessary cause of invasive cervical cancer worldwide. J Pathol 1999;189:12–9.
2. International Agency for Research on Cancer. Human papillomavirus: IARC monographs on the evaluation of carcinogenic risks to human (IARC Monographs). World Health Organization; 2007. p. 678.
3. Schlecht NF, Kulaga S, Robitaille J, et al. Persistent human papillomavirus infection as a predictor of cervical intraepithelial neoplasia. JAMA 2001;286:3106–14.
4. Schlecht NF, Platt RW, Duarte-Franco E, et al. Human papillomavirus infection and time to progression and regression of cervical intraepithelial neoplasia. J Natl Cancer Inst 2003;95:1336–43.
5. Baseman JG, Koutsky LA. The epidemiology of human papillomavirus infections. J Clin Virol 2005;32S:S16–24.
6. Wang SS, Hildesheim A. Viral and host factors in human papillomavirus persistence and progression. J Natl Cancer Inst Monogr 2003;31:35–40.
7. Fausch SC, daSilva DM, Rudolf MP, Kast WM. Human papillomavirus virus-like particles do not activate Langerhans cells: a possible immune escape mechanism used by human papillomaviruses. J Immunol 2002;169:3242–9.
8. Hazelbag S, Gorter A, Kenter GG, van den Broek L, Fleuren G. Transforming growth factor-β1 induces tumor stroma and reduces tumor infiltrate in cervical cancer. Hum Pathol 2002;33:1193–9.
9. Park JS, Kim EJ, Kwon HJ, Hwang ES, Namkoong SE, Um SJ. Inactivation of interferon regulatory factor-1 tumor suppressor protein by HPV E7 oncoprotein. Implication of the E7-mediated immune evasion mechanism in cervical carcinogenesis. J Biol Chem 2000;275:6764–9.
10. Ronco LV, Karpova AY, Vidal M, Howley PM. Human papillomavirus 16 E6 oncoprotein binds to interferon regulatory factor-3 and inhibits its transcriptional activity. Genes Dev 1998;12:2061–72.
11. Hasan UA, Bates E, Takeshita F, et al. TLR9 expression and function is abolished by the cervical cancer-associated human papillomavirus type 16. J Immunol 2007;178:3186–97.
12. Tindle RW. Immune evasion in human papillomavirus-associated cervical cancer. Nat Rev Cancer 2002;2:59–65.
13. de Jong A, van Poelgeest MIE, van der Hulst JM, et al. Human papillomavirus type 16-positive cervical cancer is associated with impaired CD4+ T-cell immunity against early antigens E2 and E6. Cancer Res 2004;64:5449–55.
14. Welters MJ, van der Logt P, van den Eeden SJ, et al. Detection of human papillomavirus type 18 E6 and E7-specific CD4+ T-helper 1 immunity in relation to health versus disease. Int J Cancer 2006;188:95–6.
15. van der Burg SH, Piersma SJ, de Jong A, et al. Association of cervical cancer with the presence of CD4+ regulatory T cells specific for human papillomavirus antigens. Proc Natl Acad Sci U S A 2007;104:12087–92.
16. Hammes LS, Tekmal RR, Naud P, et al. Macrophages, inflammation and risk of cervical intraepithelial neoplasio (CIN) progression-clinicopathological correlation. Gynecol Oncol 2007;105:157–65.
17. Mazibrada J, Ritta M, Mondini M, et al. Interaction between inflammation and angiogenesis during different stages of cervical carcinogenesis. Gynecol Oncol 2008;108:112–20.
18. Mantovani A, Sozzani S, Locati M, Allavena P, Sica A. Macrophage polarization: tumor-associated macrophages as a paradigm for polarized M2 mononuclear phagocytes. Trends Immunol 2002;23:549–55.
19. Sica A, Bronte V. Altered macrophage differentiation and immune dysfunction in tumor development. J Clin Invest 2007;117:1155–66.
20. Condeelis J, Pollard JW. Macrophages: obligate partners for tumor cell migration, invasion, and metastasis. Cell 2006;124:263–6.

21. Lewis CE, Pollard JW. Distinct role of macrophages in different tumor microenvironments. Cancer Res 2006;66:605–12.

22. Hicks AM, Riedlinger G, Willingham MC, el al. Transferable anticancer innate immunity in spontaneous regression/complete resistance mice. Proc Natl Acad Sci U S A 2006;103:7753–8.

23. Bonnotte B, Larmonier N, Favre N, et al. Identification of tumor-infiltrating macrophages as the killers of tumor cells after immunization in a rat model system. J Immunol 2001;167:5077–83.

24. Hagermann T, Lawrence T, McNeish I, et al. "Re-educating" tumor-associated macrophages by targeting NF-κB. J Exp Med 2008;205:1261–8.

25. Lin KY, Guarnieri FG, Staveley-O'Carrol KF, et al. Treatment of established tumors with a novel vaccine that enhances major histocompatibility class II presentation of tumor antigen. Cancer Res 1996;56:21–6.

26. Tseng CW, Hung CF, Alvarez RD, et al. Pretreatment with cisplatin enhances E7-specific CD8+ T Cell mediated antitumor immunity induced by DNA vaccination. Clin Cancer Res 2008;14:3185–92.

27. Tseng CW, Monie A, Wu CY, et al. Treatment with proteasome inhibitor bortezomib enhances antigen-specific CD8+ T cell mediated antitumor immunity induced by DNA vaccination. J Mol Med 2008;86:899–908.

28. Berraondo P, Nouzé C, Préville X, Ladant D, Leclerc C. Eradication of large tumors in mice by a tritherapy targeting the innate, adaptative, and regulatory components of the immune system. Cancer Res 2007;67:8847–55.

29. Maximiano FA, da Silva MA, Daghastanli KRP, de Araújo PS, Chaimovich H, Cuccovia IM. A convenient method for lecithin purification from fresh eggs. Quim Nova 2008;314:910–3.

30. Chang C, Zoghi B, Liao LC, Kuo L. The involvement of tyrosine kinases, cyclic AMP/protein kinase A, and p38 mitogen-activated protein kinase in IL-13-mediated arginase I induction in macrophages: its implications in IL-13-inhibited nitric oxide production. J Immunol 2000;165:2134–41.

31. Hibbs JB, Jr., Taintor RR, Vavrin Z, Rachlin EM. Nitric oxide: a cytotoxic activated macrophage effector molecule. Biochem Biophys Res Commun 1988;157:87–94.

32. Sapan CV, Lundlad RL, Price NC. Colorimetric protein assay techniques. Biotechnol Appl Biochem 1999;29:99–108.

33. Deamer D, Banghan AD. Large volume liposomes by an ether vaporization method. Biochim Biophys Acta 1976;443:629–34.

34. Kolloff RH, Ward HK, Ziembra VF. Precise determination of traces of pyrophosphate in orthophosphates. Anal Chem 1960;32:1687–60.

35. Rouser G, Fleischer S, Yamamoto A. Two-dimensional thin layer chromatographic separation of polar lipids and determination of phospholipids by phosphorus analysis of spots. Lipids 1970;5:494–96.

36. Komohara Y, Ohnishi K, Kuratsu J, Takeya M. Possible involvement of the M2 anti-inflammatory macrophage phenotype in growth of human gliomas. J Pathol 2008;216:15–24.

37. Miselis NR, Wu ZJ, Van Rooijen N, Kane AB. Targeting tumor-associated macrophages in an orthotopic muirine model of diffuse malignant mesothelioma. Mol. Cancer Ther 2008;7:788–99.

38. Zeni E, Mazzetti L, Miotto D, et al. Macrophage expression of interleukin-10 is a prognostic factor in nonsmall cell lung cancer. Eur Respir J 2007;30:627–32.

39. Van Ginderachter JA, Meerschaut S, Liu Y, et al. Peroxisome proliferator-activated receptor γ (PPARγ) ligands reverse CTL suppression by alternatively activated (M2) macrophages in cancer. Blood 2006;108:525–35.

40. Gabrilovich DI, Nagaraj S. Myeloid-derived suppressor cells as regulators of the immune system. Nat Rev Immunol 2009;9:162–74.

41. Niederkon JY. Emerging concepts in CD8(+)T regulatory cells. Curr Opin Immunol 2008;20:327–31.

42. Serafini P, Meckel K, Kelso M, et al. Phosphodiesterase-5 inhibition augments endogenous antitumor immunity by reducing myeloid-derived suppressor cell function. J Exp Med 2006;203:2691–702.

43. Van Rooijen N. Liposomes for targeting of antigens and drugs: immunoadjuvant activity and liposome-mediated depletion of macrophages. J Drug Target 2008;16:529–34.

44. Roelofs AJ, Thompson K, Gordon S, Rogers MJ. Molecular mechanisms of action of bisphosphonates: current status. Clin Cancer Res 2006;12:6222–30s.

45. Martinez FO, Helming L, Gordon S. Alternative activation of macrophages: an immunologic functional perspective. Annu Rev Immunol 2009;27:451–83.

46. Gabrilovich DI, Velders MP, Sotomayor EM, Kast WM. Mechanism of immune dysfunction in cancer mediated by immature Gr1+ myeloid cells. J Immunol 2001;166:5398–406.

47. Colombo MP, Piconese S. Regulatory-T-cell inhibition versus depletion: the right choice in cancer immunotherapy. Nat Rev Cancer 2007;7:880–7.

48. Billerbeck E, Thimme R. CD8+ regulatory T cells in persistent human viral infections. Hum Immunol 2008;69:771–5.

49. Wang R. CD8+ regulatory T cells, their suppressive mechanisms, and regulation in cancer. Hum Immunol 2008;69:811–4.

50. Giraudo E, Inoue M, Hanahan D. An amino-biphosphonate targets MMP-9-expressing macrophages and angiogenesis to impair cervical carcinogenesis. J Clin Invest 2004;114:623–33.

Clinical Cancer Research

HPV16 Tumor Associated Macrophages Suppress Antitumor T Cell Responses

Ana Paula Lepique, Katia Regina Perez Daghastanli, Iolanda Midea Cuccovia, et al.

Clin Cancer Res 2009;15:4391-4400.